Available online at www.sciencedirect.com
ScienceDirect
Journal of Applied Mathematics and Mechanics 70 (2006) 549–559
Journal of APPLIED MATHEMATICS AND MECHANICS
www.elsevier.com/locate/jappmathmech

Bifurcations of the precessional motion of an unbalanced rotor☆

I.A. Pasynkova

St Petersburg, Russia

Received 27 September 2005

Abstract

The loss of stability of the cylindrical and conical precession of a rigid unbalanced rotor in non-linear elastic bearings with dissipation accompanying a change in the angular velocity of rotation of the rotor is investigated. It is assumed that the rotor has four degrees of freedom. It is established, using equations of the first degree of approximation, that the loss of stability of cylindrical and conical precessions on passing through a zero root can be accompanied by the excitation of a direct synchronous precession of the hyperboloidal type. Moreover, the equation of the boundary for the onset of self-excited oscillations is obtained and it is shown by means of numerical modelling that supercritical Hopf bifurcation and a strange attractor can occur.
© 2006 Elsevier Ltd. All rights reserved.

In the analysis of the dynamics of an unbalanced rigid rotor with four degrees of freedom, the problem of the forced oscillations of a statically and dynamically unbalanced rotor in linear elastic bearings[1] and the problem of a rotor in non-linear elastic bearings, ignoring drag, has been considered and the cylindrical and conical precession parameters of a completely unbalanced rotor were obtained in Refs. 2,3.[a] The conditions for the stability of the cylindrical precession of a statically unbalanced rotor in non-linear bearings with two degrees of freedom have been found under the assumption that the rotor executes plane-parallel motion in the linear approximation[4,5] and by virtue of the complete equations.[6]

It has been established[7–9] that a statically and dynamically unbalanced rotor, mounted vertically and symmetrically (the centre of gravity is located in the middle between the bearings), in non-linear elastic bearings can execute steady motion, which is a direct synchronous precession during which the form of the precession (cylindrical, conical or hyperboloidal) is determined by the shape of the surface over which the axis of the rotor sweeps in space.

In this paper, the conditions for the loss of stability of the precessional motion of an unbalanced rotor with four degrees of freedom are investigated as a function of the angular velocity of rotation using linear analysis. The rotor is mounted in fixed non-linear elastic bearings. Quasilinear (with a cubic non-linearity) reactions of the bearings and extremely non-linear reactions of the bearings, defined by the Hertz formula, are considered. External and internal drag is taken into account. Since a state of equilibrium in a system of coordinates rotating with the angular velocity of the rotor corresponds to the direct synchronous precession of the rotor, the problem arises of studying the one-parameter bifurcation of a state of relative equilibrium.[10–12]

☆ *Prikl. Mat. Mekh.* Vol. 70, No. 4, pp. 605–616, 2006.

E-mail address: ip@ip1157.spb.edu.

[a] Also, see: *Meller AS* Dynamics of highly reversible rotary machines. Candidate Dissertation. St Petersburg, 1997.

0021-8928/$ – see front matter © 2006 Elsevier Ltd. All rights reserved.
doi:10.1016/j.jappmathmech.2006.09.006

1. Equations of motion

1.1. Direct synchronous precessions

As previously in Refs. 7–9, we consider a dynamically symmetrical rigid rotor of mass M, length L and moments of inertia J_p (axial) and J_t (equatorial). The static eccentricity is equal to e. The dynamic eccentricity is represented by the quantity δ and the phase shift by ε The rotor is made to rotate by a motor which is capable of maintaining a constant angular velocity of rotation $\bar{\Omega}$. By neglecting the displacement of the rotor along the axis of rotation, it can be treated as a mechanical system with four degrees of freedom. The Cartesian coordinates u_j, v_j ($j = 1, 2$) of the j-th end of the axis of the rotor (of the pivot) in a plane which is perpendicular to the axes of the bearings are selected as the generalized coordinates. The elastic bearings are assumed to be identical and possess central symmetry. In this case, the reaction of a bearing only has a radial component, which is equal to $\mathbf{F}_j = -F_j(|S_j|)\mathbf{n}$. Here, $S_j = u_j + iv_j$ is the displacement of the j-th pivot from the equilibrium position (in complex form) and $\mathbf{n}_j$ is a unit vector in the direction of S_j. The forces due to external drag, which are proportional to the absolute rotation rate of the pivot $\mathbf{R}_j^{(e)} = -\tilde{\mu}_e \dot{S}_j$, and the forces due to internal drag, which are proportionate to the relative velocity $\mathbf{R}_j^{(i)} = -\tilde{\mu}_i(\dot{S}_j - i\bar{\Omega}S_j)$ are taken into account.[13,14]

The equations of motion of the rotor can be obtained using theorems on the motion of the centre of mass and the change in the angular momentum with respect to the centre of mass.[1,2] We now introduce a characteristic linear dimension h, for example, $2e$ or $L\delta$, into the treatment and a characteristic angular velocity ω_0, the choice of which depends on the function F_j. In complex form, after changing to the dimensionless variables $s_j = S_j/h$, $\tau = \omega_0 t$ and the dimensionless angular velocity $\Omega = \bar{\Omega}/\omega_0$, the equations of motion take the form

$$\begin{aligned}
&\ddot{s}_1 + \ddot{s}_2 + (\mu_e + \mu_i)(\dot{s}_1 + \dot{s}_2) - i\Omega\mu_i(s_1 + s_2) + \\
&+ f_1(|s_1|)\frac{s_1}{|s_1|} + f_2(|s_2|)\frac{s_2}{|s_2|} = d_1\Omega^2\exp(i\Omega\tau) \\
&\ddot{s}_2 - \ddot{s}_1 + ((\mu_e + \mu_i)kl - i\Omega\lambda)(\dot{s}_2 - \dot{s}_1) - i\Omega\mu_i kl(s_2 - s_1) + \\
&+ kl\left(f_2(|s_2|)\frac{s_2}{|s_2|} - f_1(|s_1|)\frac{s_1}{|s_1|}\right) = (1-\lambda)d_2\Omega^2\exp(i(\Omega\tau - \varepsilon))
\end{aligned} \tag{1.1}$$

Here $f_j(|s_j|) = 2F_j(h|s_j|)/(hM\omega_0^2)$ and differentiation is carried out with respect to the dimensionless variable τ. The remaining parameters, which can be called structural parameters, have the following meaning

$$\begin{aligned}
&k = \frac{ML^2}{4(J_t - J_p)}, \quad \lambda = \frac{J_p}{J_t}, \quad l = 1 - \lambda, \quad d_1 = \frac{2e}{h}, \quad d_2 = \frac{L\delta}{h} \\
&\mu_e = \frac{2\tilde{\mu}_e}{M\omega_0}, \quad \mu_i = \frac{2\tilde{\mu}_i}{M\omega_0}
\end{aligned} \tag{1.2}$$

In the case of a dynamically prolate body ($\lambda < 1$), the parameter $k > 0$, and, in the case of a dynamically oblate body ($\lambda > 1$), we have $k < 0$ since $kl > 0$

System (1.1) admits of a solution of the form

$$s_j = R_j\exp(i\varphi_j)\exp(i\Omega\tau), \quad j = 1, 2 \tag{1.3}$$

where R_j, φ_j are real constants and $R_j > 0$. The quantity R_j is the radius of the circular orbit of the j-th pivot and φ_j is the phase shift with respect to the perturbing force.

The solution (1.3) is a direct synchronous precession of the rotor. If $\varphi_1 = \varphi_2$ and $R_1 = R_2$, then cylindrical precession (CyP) occurs. If $\varphi_1 = \varphi_2$ or $\varphi_1 = \varphi_2 + \pi$ for any R_1, R_2, then conical precession (CoP) occurs. If, however, $\varphi_1 \neq \varphi_2$ and $R_1 \neq R_2$, then the precession will be hyperboloidal. It is easy to see that CyP ($s_1 = s_2$) can only occur in the case of a dynamically balanced rotor ($\delta = 0$) since, in this case, the second equation of (1.1) is satisfied identically. In its turn, symmetric conical precession (SCoP), for which $s_1 = -s_2$, can only occur in the case of a statically balanced rotor ($e = 0$) since, in this case, the first equation of system (1.1) is satisfied identically.

Substituting solution (1.3) into system (1.1), we obtain a linear inhomogeneous system of algebraic equations in the quantities $\exp(i\varphi_j)$ ($j=1, 2$) and, solving this system, we obtain

$$\exp(i\varphi_j) = \frac{\Omega^2}{R_j\Delta_{res}}(d_1(B_{3-j}+ik\mu_e\Omega)+(-1)^j d_2(A_{3-j}+i\mu_e\Omega)\exp(-i\varepsilon))$$

$$\Delta_{res} = \Delta - 2k\mu_e^2\Omega^2 + i\mu_e\Omega\sum_{j=1,2}(kA_j+B_j)\neq 0 \tag{1.4}$$

$$\Delta = A_1B_2+A_2B_1;\quad A_j = \frac{f_j(R_j)}{R_j}-\Omega^2;\quad B_j = k\frac{f_j(R_j)}{R_j}-\Omega^2$$

The set $\Delta=0$ defines the set of *non-linear resonances* in the space $\{R_1, R_2, \Omega^2\}$, and its role is similar to a skeleton curve in an amplitude-frequency characteristic (AFC) in the Duffing equation. This set is unattainable for any finite values of the frequency whatsoever in the case of a statically and dynamically unbalanced rotor which is rotating without drag [7]. It will be shown that instability in the direct synchronous precession arises close to this set.

The property $|\exp(i\varphi_j)|=1$ enables us to obtain a system for determining the quantities R_j and it is then also possible to find the phases φ_j. We note that all of the quantities which have been obtained up to this point, that is, $\exp(i\varphi_j)$, Δ_{res}, Δ, R_j and φ_j, are independent of the internal drag coefficient μ_j. The equation

$$\left|\exp(i(\varphi_1-\varphi_2))\right| = 1 \tag{1.5}$$

defines an integral set in the space $\{R_1, R_2, \Omega^2\}$ to which only states of relative equilibrium of system (1.1) can belong. In the case of a rotor which has one form of unbalancing, the set (1.5) includes the plane $R_1=R_2$ and a certain surface which is symmetrical about this plane. The equilibrium states, which parametrize a CyP or a SCoP are localized in the plane $R_1=R_2$. Henceforth, we shall study cylindrical and symmetrical conical direct synchronous precessions.

Standard linear analysis can be used to investigate the stability of the resulting direct synchronous precession processes. The system of variational equations for CyP and SCoP (of the eighth order) is separated into two independent fourth-order subsystems, and the characteristic polynomial is therefore represented in the form of a product of the fourth-power polynomials P_1 and P_2.[8,9] The boundaries of loss of stability are determined by the appearance of zero or pure imaginary roots, which corresponds to the free terms of these polynomials or the third-order Hurwitz determinants vanishing.

Elementary catastrophe theory[12] can be used to study the bifurcation points, for which the stability matrix has a single zero root. The investigation of points of bifurcation, where there is a single pair of pure imaginary roots, is carried out numerically.

2. Bifurcations of a cylindrical precession

2.1. The amplitude–frequency characteristic of a CyP

Consider a statically unbalanced rotor ($e\neq 0, \delta=0$), fixed in quasilinear elastic mountings with a cubic non-linearity. Suppose the reaction force is specified in the form

$$F_j = -(a_0+a_1|S_j|^2)S_j,\quad j=1,2$$

where a_0, a_1 are coefficients which characterize the elastic properties of the mountings. Here it is convenient to choose $h=2e$, $\omega_0^2=2a_0/M$ and to change to the new variables $x=\Omega^2$, $y_j=R_j^2$.

Among the solutions (1.3), it is possible to pick out the solution $s_1=s_2$ corresponding to a CyP. But, among the solutions (1.3), there are also some such that $y_1\neq y_2$.

The equation of the surface (1.5) takes the form

$$y_1B_1^2 - y_2B_2^2 + (y_2-y_1)k^2\mu_e^2x = 0 \tag{2.1}$$

or

$$(y_2 - y_1)[L_2(x, y_1, y_2) + L_1(x, y_1, y_2) + k^2 + k^2\mu_e^2 x] = 0$$

$$L_2(x, y_1, y_2) = x^2 + k^2c^2(y_1^2 + y_2^2 + y_1y_2) - 2kcx(y_1 + y_2)$$

$$L_1(x, y_1, y_2) = -2kx + 2k^2c(y_1 + y_2); \quad c = 4e^2a_1/a_0$$

When $\mu_e = 0$, this set is the plane $y_1 = y_2$ and a non-right elliptic cone with vertex at the point $\{k, 0, 0\}$, and this cone touches the plane $\{x, y_j\}$ along the line $B_{3-j} = 0$ ($j = 1, 2$) An ellipse in the section of the cone with a plane $x = \text{const}$. is orientated such that one of its axes is directed along the bisector of the coordinate angle. When $\mu_e \neq 0$, the surface (2.1) takes the form of a plane $y_1 = y_2$ and a sheet of a two-sheet elliptic hyperboloid

$$L_2(x, y_1, y_2) + L_1(x, y_1, y_2) + k^2 + k^2\mu_e^2 x = 0 \tag{2.2}$$

which asymptotically approximates to a cone when $\mu_e \to 0$. The hyperboloid (2.2) and the plane $y_1 = y_2$ intersect along the hyperbola

$$(k(1 + cy) - x)(k(1 + 3cy) - x) + k^2\mu_e^2 x = 0; \quad y = y_1 = y_2 \tag{2.3}$$

which, when $\mu_e = 0$, degenerates into its pair of asymptotes.

The set of non-linear resonances degenerates into $A_1B_1 = 0$ and is represented by the two straight lines $(1 + cy - x)(k(1 + cy) - x) = 0$. The amplitude-frequency and phase-frequency characteristics of a CyP have the form

$$\sqrt{y((1 + cy - x)^2 + \mu_e^2 x)} - \frac{1}{2}x = 0, \quad \operatorname{tg}\varphi = -\frac{\mu_e\sqrt{x}}{1 + cy - x} \tag{2.4}$$

In the case of a fairly small external drag ($\mu_e \leq \sqrt{c}/2$) or when there is no drag ($\mu_e = 0$), the amplitude-frequency characteristic (AFC) consists of two branches which do not have common points with the resonance line $1 + cy - x = 0$.[15]

Self-centring of the rotor occurs and the limit value when $x \to \infty$ is equal to $y_\infty = 1/4$. This corresponds to the fact that the radius of a CyP is exactly equal to the eccentricity e, that is, the rotor rotates in such a way that its centre of mass tends to occupy a position on the axis of the bearings.

An AFC is shown in Fig. 1a, for a dynamically prolate rotor ($\lambda < 1$, $k > 0$) and the following values of the structural parameters

$$k = 0.6, \quad l = 0.3, \quad c = 0.25, \quad \mu_e = 0.3, \quad \mu_i = 0.4 \tag{2.5}$$

The limit value of $y = y_\infty$ is shown (the dash-dot line).

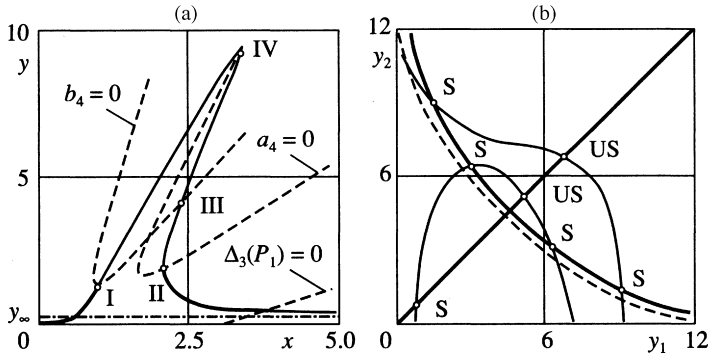

Fig. 1.

2.2. The stability of a CyP

The coefficients of the characteristic polynomial P_2 for the second equation of system (1.1) have the form

$$b_0 = 1, \quad b_1 = 2kl\mu, \quad b_2 = 2kl(1+2cy) + (l^2+1)x + k^2l^2\mu^2$$
$$b_3 = 2k^2l^2\mu(1+2cy) + 2kl(\mu_e - l\mu_i)x \tag{2.6}$$
$$b_4 = l^2((k(1+cy)-x)(k(1+3cy)-x) + k^2\mu_e^2 x); \quad \mu = \mu_e + \mu_i$$

The coefficients $a_0, a_1, \ldots, a_4$ of the polynomial P_1 for the first equation are determined using the corresponding formulae (2.6) when $k = l = 1$.

The conditions for a transition through zero roots

$$a_4 = (1+cy-x)(1+3cy-x) + \mu_e^2 x = 0$$
$$b_4 = (k(1+cy)-x)(k(1+3cy)-x) + k^2\mu_e^2 x = 0 \tag{2.7}$$

are independent of the internal drag coefficient μ as is also the amplitude curve (2.4). It can be seen from conditions (2.7) that instability occurs close to the non-linear resonances

$$A_1 = 1 + cy - x = 0, \quad B_1 = k(1+cy) - x = 0$$

Each of conditions (2.7) represents a hyperbola in the plane $\{x, y\}$ and each resonance line is one of the asymptotes of these hyperbolae. The second condition of (2.7) for a transition through a zero root and condition (2.3) for the branching of the integral set are identical.

It can be shown that, when internal drag is ignored, the conditions of the Routh-Hurwitz criterion are only violated when $\{a_4 \le 0\} \cup \{b_4 \le 0\}$, that is, loss of stability can only occur as a result of passing through zero roots of the characteristic determinant. It can be concluded from this that the process of self-centring of the rotor at high angular velocities is asymptotically stable.

When there is internal drag, if $\mu_i > \max(\mu_e, \mu_e/l)$, the coefficients a_3 and b_3 become negative for fairly large values of x and bounded values of y. Moreover, when $a_4 > 0$ and $b_4 > 0$, the inequalities $a_3 < 0$, $b_3 < 0$ imply the inequalities

$$\Delta_3(P_1) = -a_1^2 a_4 - a_3^2 a_0 + a_1 a_2 a_3 < 0$$
$$\Delta_3(P_2) = -b_1^2 b_4 - b_3^2 b_0 + b_1 b_2 b_3 < 0$$

that is, at high angular velocities, the process of self-centring of the rotor becomes unstable.

The boundaries of the transition through zero roots $a_4 = 0$, $b_4 = 0$ and through pure imaginary roots are also shown in Fig. 1a (the dashed curves). When $l = 0.3$, the inequalities $\Delta_3(P_2) > 0$, $b_3 > 0$ hold for all x and the boundary of the transition through pure imaginary roots has the form

$$\Delta_3(P_1) = c^2y^2 + 2cy(4x + \mu^2) - (4x + \mu^2)((\mu_i/\mu)^2 x - 1) = 0 \tag{2.8}$$

This curve is a part of a branch of a hyperbola which is approximated to a high accuracy by its asymptote $y = ((\mu_i/\mu)^2 x - 1)/(2c)$. The segments of the asymptotically stable states of the amplitude curve are shown by the solid line. The parameters were chosen in such a way that the curves $a_4 = 0$, $b_4 = 0$ and the AFC did not intersect at a point (thereby excluding the case of multiple zero roots).

2.2.1. Bifurcation of a CyP on passing through a zero root

System (1.1) will be autonomous in a rotating system of coordinates, and elementary catastrophe theory[12] can be used to study the behaviour of the system in the segment $\{a_4 \le 0\} \cup \{b_4 \le 0\}$. The curves $a_4 = 0$ and $b_4 = 0$ in the $\{x, y\}$ plane form a bifurcation set, and points *I–IV* of the intersection of the curves with the AFC are degenerate critical points or "non-Morse " critical points (Fig. 1a). A change in a parameter causes a qualitative change in the behaviour of the system in the neighbourhood of a degenerate critical point. The splitting of the degenerate point into a number of non-degenerate points ("morsification") and their localization changes, during which, when a parameter is varied

in one direction, a degenerate point splits into three isolated "non-Morse" points and, when the parameter is varied in the other direction, the number of singular points does not change but the point ceases to be degenerate.

As a result, it is easy to follow how the loss of stability of a CyP occurs over a range of frequencies from point *I* to point *IV*. When the frequency increases, the degenerate point *I* splits into three non-degenerate points, the CyP becomes unstable and two stable states of direct synchronous precession, which are localized on the surface of the two-sheet hyperboloid (2.2), appear. These precessions are no longer cylindrical. When the frequency increases further and on passing through the critical point *II*, it, in turn, also splits into three non-degenerate points. The overall number of equilibrium states attained is five for which three different cylindrical precession processes are possible (two of them are unstable and one is asymptotically stable). When the frequency increases further and on passing through the degenerate point *III*, further splitting occurs during which the number of different cylindrical precession processes remains equal to three, two of which are unstable while the one with the minimum amplitude is asymptotically stable. The number of different precessions of a non-cylindrical type reached four. Finally, on passing through point *IV*, the number of non-degenerate points falls to two. There is a single asymptotically stable cylindrical precession process and four direct synchronous precession processes of a non-cylindrical type.

In the case of a fixed frequency, the radii of the orbits of the pivots are found as the points of intersection of curve (1.5) and the curve

$$\left|\exp(i\varphi_1)\right| = 1 \tag{2.9}$$

(or the curve $|\exp(i\varphi_2)| = 1$) and the phases satisfy the relation

$$\operatorname{tg}(\varphi_1 - \varphi_2) = \frac{k\mu_e\sqrt{x}(B_1 - B_2)}{B_1B_2 + k_2\mu_e^2 x}$$

Consequently, the equilibrium states, localized on the hyperboloid (2.2) are precessions of a hyperboloidal type since, for unequal radii of the orbits of the pivots, their phases are not identical and do not differ by π.

Sections of the surface (1.5) when $\mu_e \neq 0$ (the solid line) and when $\mu_e = 0$ (the dashed line) are shown in Fig. 1b for $x = 2.6$, curve (2.9) is represented by the fine curve and the equilibrium states (S is stable and US is unstable) are shown by the open circles. There are three equilibrium states corresponding to a CyP, located on the bisector and four asymptotically stable equilibrium states, which correspond to an asymmetrical hyperboloidal precession. Numerical verification confirmed that all the roots of the characteristic equation for these points have negative real parts.

2.3. Hopf bifurcation

2.3.1. Strange attractor

The equation $\Delta_3(P_1) = 0$ also defines a bifurcation set in the $\{x, y\}$ plane. At the point of intersection of this curve and the AFC, the characteristic polynomial $P_1 = 0$ has a single pair of pure imaginary roots. Depending on the sign of the Lyapunov exponent, the bifurcation can be one of two types[10,11]: the "soft" type, when the loss of stability is accompanied by the evolution of a stable limit cycle, and the "hard" type, when loss of stability occurs as a consequence of merging with a previously existing unstable limit cycle. Numerical integration of system (1.1) shows that, in the case of the structural parameters (2.5), "soft" excitation of the natural oscillations (supercritical Hopf bifurcation[12]) occurs.

The point of the amplitude curve, where the pair of pure imaginary roots appears, then has the coordinates ($x = 3.8$, $y = 0.48$) (Fig. 1a). The limit cycle in the $\{R_1, \dot{R}_1\}$ plane of the phase space $\{R_1, \dot{R}_1, R_2, \dot{R}_2, \varphi_1 - \varphi_2, \dot{\varphi}_1 - \dot{\varphi}_2\}$ is shown in Fig. 2 for the value $x = 6(\Omega = \sqrt{6})$. This graph corresponds to 20 revolutions of the rotor under steady conditions (after 180 revolutions). The periodic motion, which is parametrized by this limit cycle, is a CyP since, at the same time, $\varphi_1 - \varphi_2 = 0$. The limit cycle for the second pivot (in the $\{R_2, \dot{R}_2\}$ plane) has the same form.

In a study of a statically unbalanced rotor, held in quasilinear elastic mountings, within the framework of the model of a rotor with two degrees of freedom, a method was proposed in Ref. 16 for finding the self-excited oscillations, and, following this method, we shall seek the self-excited oscillations in the form

$$s_j = r_j\exp(i(\omega\tau + \psi)) + R_j\exp(i(\Omega\tau + \varphi_j)) \tag{2.10}$$

where r_j, R_j, φ_j, ψ, ω are unknown quantities. The representation of the self-excited oscillations in such a form enables us to separate out, in a solution with an unknown period, the component which has the period of the external perturbing force. Substituting expression (2.1) into Eq. (1.1) and averaging over the period $2\pi/(\Omega-\omega)$, we obtain approximate equations in the unknowns r_j, R_j, φ_j, ω which will be independent of ψ. These equations have the solutions

$$r_1 = r_2 = r, \quad R_1 = R_2 = R, \quad \varphi_1 = \varphi_2 = \varphi$$

To determine the unknowns ω, r, R, φ, we obtain the following approximate equations

$$\begin{aligned} &\mu\omega - \mu_i\Omega = 0, \quad c(r^2 + 2R^2) + 1 - \omega^2 = 0 \\ &R(kc(2r^2 + R^2) + k - \omega^2)\sin\varphi + k\mu_e R\Omega\cos\varphi = 0 \\ &R(kc(2r^2 + R^2) + k - \omega^2)\cos\varphi - 2k\mu_e R\Omega\sin\varphi = \Omega^2/4 \end{aligned} \tag{2.11}$$

From the first equation of system (2.11), we find the value of ω which enables one to determine the period of the self-excited oscillations approximately in terms of the time of a single revolution of the rotor T_r:

$$\omega = \frac{\mu_i}{\mu}\Omega, \quad T \approx \frac{\mu}{\mu_e}\frac{2\pi}{\Omega} = \frac{\mu}{\mu_e}T_r \tag{2.12}$$

The limit cycle, constructed using the approximate equations (2.11), is shown by the dashed curve in Fig. 2. Quite good agreement (an error of ≈2.5%) is observed between the exact and approximate solutions for the maximum values of the deviations which is most important. The error in determining the period of the self-excited oscillations is approximately 6.5%. It should be noted, however, that the accuracy of the approximate values falls as Ω increases.

Numerical integration of system (1.1) was carried out over the range of frequencies $x \in [4, 10]$ ($\Omega \in [2, 3.16]$) which showed that stable self-excited oscillations with a period close to the value T exist for all frequencies from this range but, for certain frequency values, their attraction domain is extremely restricted. For instance, in the range $x \in (4.3, 7.7)$ ($\Omega \in (2.07, 2.77)$), the self-excited oscillations became sensitive to a change in the initial data and, together with the T-periodic motion, the existence of other attractors was revealed.

During the integration, only the initial values of R_j were changed for each frequency, and the initial values of the remaining variables were taken to be equal to zero. The 5×5 square with respect to R_1, R_2 was subdivided into 1×1 elements. In the AFC (Fig. 1a), the maximum value $y_{\max} \approx 9.25$ or $R_{1\max} = R_{2\max} \approx 3.04$ and, consequently, the range of variation of the initial data was quite wide. Within each element, a point was randomly chosen, except for the diagonal elements where a value was chosen on the diagonal but also randomly. Integration with respect to time was carried out for up to 500 revolutions of the rotor. The numerical experiment showed that, for frequencies in the range $x \in (4.3, 7.7)$, a further $2T$-periodic limit cycle exists which parametrizes a hyperboloidal precession of complex structure. If the initial values are chosen to be symmetric (equal) or very close to it, then the trajectory tends to self-excited oscillations with a period close to T and the process is established quite rapidly (no more than 20 revolutions of the rotor). If the initial data which are chosen are not equal, then the trajectory tends to self-excited oscillations with a period close to $2T$.

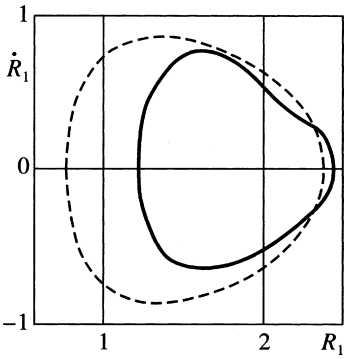

Fig. 2.

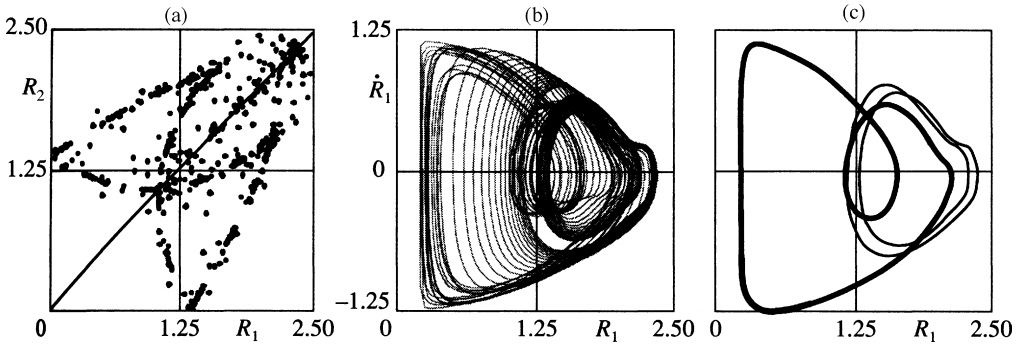

Fig. 3.

A typical implementation of the process $R_1(\tau)$ looks as follows. In the initial stage (apart from the very first revolutions), the trajectory in the $\{R_1, \dot{R}_1\}$ plane is close to a T-periodic limit cycle. A doubling of the period then occurs and the trajectory splits into two branches (one within the limit cycle and the other outside it). Then the motion "slides down" into chaotic motion (a "strange attractor" is observed) after which synchronization occurs and a $2T$-periodic limit cycle is established. As the difference in the initial values $|R_1 - R_2|$ increases, the first two phases of the process become smaller (or disappear altogether) and the time of the chaotic motion increases. For certain versions, the process was not fully established even after 700 revolutions.

A strange attractor in the (R_1, R_2) plane ($\tau = 0[\mathrm{mod}(2\pi/\Omega)]$) for $x = 6$ and the initial values $R_1 = 2.427$, $R_2 = 1.321$ is shown in Fig. 3a. Synchronization is distinctly visible, that is, the existence of a quasiperiodic solution which is parametrized by two-loop limit cycle.

The phase trajectory in the $\{R_1, \dot{R}_1\}$ plane is shown in Fig. 3b for the same frequency and initial values. This phase trajectory reflects the chaotic motion of the first pivot in the time interval of 80 to 200 revolutions of the rotor. A tow-loop limit cycle (the thick curve) is shown in Fig. 3c. The curve corresponds to a time from 450 to 500 revolutions of the rotor. The second phase of the motion from 50 to 70 revolutions is represented by the thin curve when a doubling of the period occurred and a second loop appeared in the limit cycle. In the first stage (up to 40–45 revolutions) the motion occurred close to a single-loop limit cycle (Fig. 2).

It is interesting to follow the evolution of the two-loop limit cycle in the range of frequencies where it exists. On creation ($x \approx 4.3$) the two loops of the cycle are close to one another as though they encompass the limit cycle, which has existed up to this point, from within and without. Then, when the frequency increases, the inner loop gradually contracts and the outer loop expands, and, finally, the inner loop disappears ($x \approx 7.7$) and a single-loop limit cycle is established.

3. Bifurcation of a symmetrical conical precession

We will now consider a dynamically unbalanced rotor ($e = 0$, $\delta \neq 0$) and the reaction forces, which are given by Hertz formula

$$F_j = -a_0 |S_j|^{1/2} S_j, \quad j = 1, 2$$

It is convenient to choose

$$h = L\delta, \quad \omega_0^2 = 2a_0\sqrt{L\delta}/M$$

and to change to the new variables

$$x = \Omega^2, \quad y_j = \sqrt{R_j}$$

The set (1.5) in the $\{x, y_1, y_2\}$ space represents a plane $y_1 = y_2$ and a cone ($\mu_e = 0$) or the sheet of a two-sheet hyperboloid ($\mu_e \neq 0$). Sections of the surface (1.5) are shown in Fig. 4a for ($\mu_e \neq 0$) (the thick line) and ($\mu_e = 0$) (the dash-dot line).

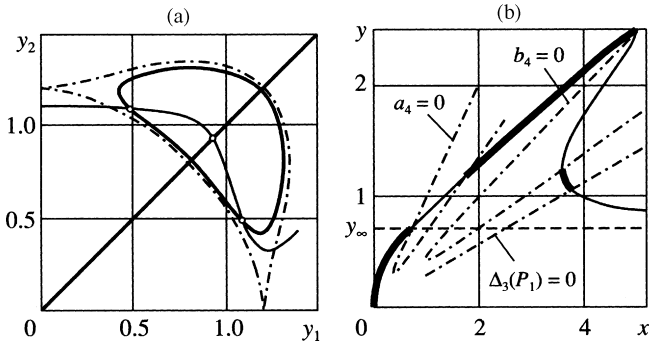

Fig. 4.

We will now consider an SCoP when

$$y_1 = y_2 = y, \quad \varphi_1 = \varphi, \quad \varphi_2 = \varphi + \pi$$

The resonance set $\Delta = 0$ represents two intersecting straight lines $(y - x)\,(ky - x) = 0$. The amplitude-frequency and phase-frequency characteristics have the form

$$y^2\sqrt{(ky-x)^2 + k^2\mu_e^2 x} - \frac{1}{2}x = 0, \quad \operatorname{tg}\varphi = -\frac{k\mu_e\sqrt{x}}{ky-x} \tag{3.1}$$

The self-centring of the rotor when $x \to \infty$ is determined by the value $y = y_\infty = 1/\sqrt{2}$. This means that the rotor rotates such that its axis of dynamic symmetry tends to occupy a position which coincides with the axis of the bearings.

The amplitude curve of a SCoP dynamically prolate rotor for

$$k = 2, \quad l = 0.3, \quad \mu_e = 0.09, \quad \mu_i = 0.13$$

is shown in Fig. 4b, where the limit value $y = y_\infty$ is shown by the dashed line.

For given l, we have $\Delta_3(P_2) > 0$, $b_3 > 0$ for all x, and the conditions for passing through zero and pure imaginary roots

$$a_4 = (y-x)(3y-2x) + 2\mu_e^2 x = 0$$

$$b_4 = (ky-x)(3ky-2x) + 2k^2\mu_e^2 x = 0 \tag{3.2}$$

$$\Delta_3(P_1) = y^2 + 80xy - 64(\mu_i/\mu)^2 x^2 + 20\mu^2 y - 16\mu_i^2 x = 0$$

are shown by the dash-dot lines in Fig. 4b. Asymptotically stable processes are represented by the thick segments of the amplitude curve.

The radii of the orbits of the pivots can be found for a specific frequency x from the range $a_4 < 0$ as the points of intersection of the curve (1.5) with the curve (2.9), and the quantities φ_1 satisfy the relation

$$\operatorname{tg}(\varphi_1 - \varphi_2) = \frac{\mu_e\sqrt{x}(A_1 - A_2)}{A_1 A_2 + \mu_e^2 x} \tag{3.3}$$

Consequently, the stable processes in this range are precessions of a hyperboloidal type. Curve (2.9) is shown by the thin line in Fig. 4a, and the equilibrium states (an unstable equilibrium state in the bisector and two stable equilibrium states arranged symmetrically about the bisector) are shown by the open circles.

For the chosen values of the structural parameters, the critical point, where there is one pair of pure imaginary roots of the equation $P_1 = 0$, has the coordinates $(x_{\text{bif}} = 3.775,\ y_{\text{bif}} = 1.051)$ (Fig. 4b).

The limit cycle for the first pivot in the $\{R_1, \dot{R}_1\}$ plane of the six-dimensional phase space $\{R_1, \dot{R}_1, R_2, \dot{R}_2, \varphi_1 - \varphi_2, \dot{\varphi}_1 - \dot{\varphi}_2\}$ is constructed in Fig. 5 for the value $x = 5$ (or $\Omega = \sqrt{5}$). The graph corresponds to twenty revolutions of

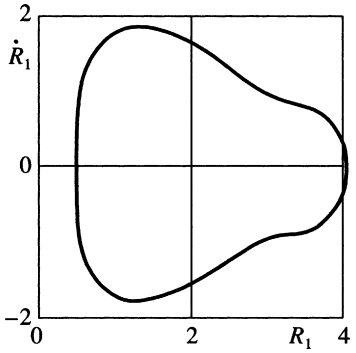

Fig. 5.

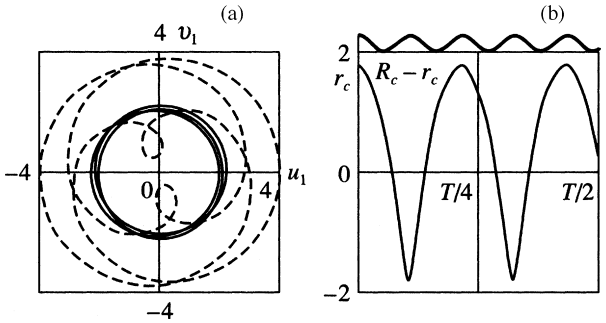

Fig. 6.

the rotor under steady conditions (after 180 revolutions) and it is practically symmetrical about the abscissa. The limit cycle for the second pivot (in the $\{R_2, \dot{R}_2\}$ plane) has precisely the same form.

The trajectories of the centre of mass of the rotor (the thick curve) and one of the pivots (the dashed curve in a plane perpendicular to the axis of the bearings, that is, in the $\{u_1, v_1\}$ u_1, v_1 plane (r_c are dimensionless Cartesian coordinates) are shown in Fig. 6a and the displacement of the centre of mass r_c relative to the axis of the bearings (the thick curve) and the displacement $(R_1 - r_c)$ of one of the pivots relative to the centre of mass (the thin curve) in the time interval $T/2 = \pi/\Omega$, which corresponds to a half revolution of the rotor, are shown in Fig. 4b. Hence it can be concluded that the self-excited oscillations represent a composition of high-frequency, close to harmonic, oscillations of the centre of mass with a small amplitude about a certain mean value and conical oscillations with respect to the centre of mass with a frequency of approximately half the value.

A numerical experiment showed that, as the angular velocity of the rotor becomes higher, the frequency of the oscillations of the centre of mass increases. The mean value of the displacement of the centre of mass also increases significantly and the amplitude of the oscillations of the centre of mass, the build up of the conical oscillation of the rotor with respect to the centre of mass and the difference in the phases decrease. For instance, for an angular velocity of rotation of the rotor $\Omega = 3\sqrt{2}(x = 18)$, the frequency of the oscillations of the centre of mass reaches a value of 17.5, the displacement of the centre of mass varies within the limits $39.34 < r_c < 39.42$ and the deviation of the pivots from the centre of mass and the phase difference satisfy the inequalities

$$|R_j - r_c| < 2.4, \quad |\varphi_1 - \varphi_2| < 0.36$$

Hence, in character, the motions of the self-excited oscillations approach a cylindrical precession during which the angular velocity of this precession increases.

References

1. Timoshenko SP. *Vibrations Problems in Engineering*. Toronto: Van Nostrand; 1955.
2. Kel'son AS, Tsimanskii YuP, Yakovlev VI. *The Dynamics of Rotors in Elastic Mountings*. Moscow: Nauka; 1982.

3. Kel'son AS, Meller AS. Dynamics of a statically unbalanced rotor in bearing mountings. *Dokl Akad Nauk SSSR* 1991;**318**(1):69–72.
4. Merkin DP. The stability of the steady motions of the axis of a rotating rotor mounted in non-linear bearings. *Prikl Mat Mekh* 1983;**47**(3):378–84.
5. Merkin DP. *Introduction to the Theory of the Stability of Motion*. Moscow: Nauka; 1987.
6. Rumyantsev VV. The stability of the steady motions of systems with quasicyclic coordinates. *Prikl Mat Mekh* 1986;**50**(6):918–27.
7. Pasynkova IA. Hyperboloidal precession of a rotor in non-linear elastic mountings. *Vestnik St Peterburg Univ Ser 1* 1997;**4**:88–95.
8. Pasynkova IA. The stability of the conical precession of a rigid unbalanced rotor. *Vestnik St Peterburg Univ Ser 1* 1998;**4**:82–6.
9. Arkhipova IM, Pasynkova IA. Investigation of the precessional motion of an unbalanced rotor. In Second Polyakov Lectures. Collected Papers. St Petersburg: Izd. Nauchn Issled Inst St Peterburg Univ; 2000: 65–72.
10. Arnol'd VI. *Additional Chapters of the Theory of Ordinary Differential Equations*. Moscow: Nauka; 1978.
11. Neimark YuI, Landa PS. *Stochastic and Chaotic oscillations*. Moscow: Nauka; 1987.
12. Gilmore R. *Catastrophe Theory for Scientist and Engineers*. N.Y.: Wiley; 1981.
13. Dimentberg FM. *Flexural Oscillations of Rotating Shafts*. Moscow: Izd Akad Nauk SSSR; 1959.
14. Bolotin VV. *Non-conservative Problems in the Theory of Elastic Stability*. Moscow: Fizmatgiz; 1961.
15. Genta G. *Vibration of Structure and Machines: Practical Aspects*. Berlin: Springer; 1999. p. 599.
16. Tondl A. *Some Problems of Self-Exited Vibrations of Rotors*. Praha: Publ. SNTL; 1974.

Translated by E.L.S.